

Sequence Effects on the Conformational Properties of the Amyloid $\beta(1-28)$ Peptide: Testing a Proposed Mechanism for the $\alpha \rightarrow \beta$ Transition[†]

Kent Kirshenbaum[‡] and Valerie Daggett*

Department of Medicinal Chemistry, BG-20, University of Washington, Seattle, Washington 98195

Received August 24, 1994; Revised Manuscript Received March 6, 1995[®]

ABSTRACT: Molecular dynamics simulations have been used to successfully reproduce the observed pH-dependent conformational properties of the amyloid $\beta(1-28)$ peptide [Kirshenbaum and Daggett (1995) *Biochemistry*, 34, 7629–7639]. On the basis of these simulations a mechanism was proposed for the unfolding of the N-terminal portion of the peptide at neutral pH when beginning from the helical conformation. It was proposed that interactions between the side chains of Ser 8 and Glu 11 are important in determining the pH dependence of the helix content. Here we further investigate this proposed mechanism and the residues involved in the conformational transition by performing computational “mutagenesis” studies. On the basis of simulations of the mutant peptides, the importance of the Ser 8–Glu 11 interaction is substantiated, and further details of the conformational transition are elucidated.

Molecular dynamics simulations of the $\beta(1-28)$ peptide reproduce the experimentally observed pH-dependent conformational properties of this peptide (Kirshenbaum & Daggett, 1995). Both the simulations and experimental studies, involving circular dichroism and nuclear magnetic resonance spectroscopies (Barrow & Zagorski, 1991; Barrow et al., 1992; Zagorski & Barrow, 1992), suggest that the peptide adopts a mixture of α -helical and random coil conformations at low pH. Loss of helical structure is observed at medium pH, with the formation of β -structure, and helical content is regained at high pH. The hypothesis based on these findings is that the conversion of α -helical structure to random coil conformations and β -structure may be an early step in β -sheet formation and subsequent plaque formation. However, studies of this peptide are not only of interest because of what they may tell us about the etiology of Alzheimer's disease. This peptide is also a good model for the elucidation of forces that determine peptide structure and dynamics.

On the basis of simulations of the β -peptide under different pH conditions (Kirshenbaum & Daggett, 1995), we suggested that the interaction between residues Ser 8 and Glu 11 was critical for interrupting the helix and triggered the subsequent unfolding of the N-terminus (Figure 1). At low pH, the α -helix content is high and Ser 8 and Glu 11 do not interact. Upon deprotonation of Glu 11 at medium pH, Ser 8 and Glu 11 interact strongly, and a kink is induced into the helix followed by unwinding of the N-terminus, yielding a single helix now beginning at Glu 11. At high pH, the two residues interact strongly, which introduces a kink into the helix but the N-terminus does not unfold. There is experimental evidence for a kink in the structure at low pH and indirect support for unwinding of the N-terminus at medium pH and

a helix–kink–helix conformation at high pH [see Kirshenbaum and Daggett (1995) for further discussion]. The ability to easily distort the main chain at Gly 9 appeared to be important in allowing the formation of the kink and subsequent tight interactions between Ser 8 and Glu 11.

In an effort to further characterize the behavior of the N-terminus of the peptide, we have conducted molecular dynamics simulations of four analogs of $\beta(1-28)$ that contain mutations at Ser 8, Gly 9, and Glu 11. All simulations were begun with an entirely α -helical structure and therefore specifically monitor the effect(s) of particular mutations on the helical state and conformational transitions from that state. Given that experimental data do not exist for these analogs, more extensive conformational sampling of non-helical conformations, as was performed in the preceding paper, is not warranted. The simulations presented here show that, by perturbing the ability of these side chains to interact, we were able to substantially alter the manner in which these “simulated mutants” respond to changes in pH. The results are also discussed in the context of current notions regarding the ability of “capping sequences” such as Ser-X-X-Glu to simultaneously stabilize the N-terminus of helices while inhibiting propagation of helical structure.

METHODS

One of four amino acid substitutions was made in the sequence of the $\beta(1-28)$ peptide (DAEFRHDSGYEVHH-QKLVFFAEDVGSNK): Ser 8 \rightarrow Ala; Gly 9 \rightarrow Ala; Glu 11 \rightarrow Gln, and Glu 11 \rightarrow Asp. Different pH conditions were modeled by adjustment of the ionization states of the relevant side chains corresponding to low, medium, and high pH (pH 2–4, 5–6, and 8–9, respectively) and are discussed in the preceding paper (Kirshenbaum & Daggett, 1995). Carboxylate side chains were protonated at low pH, and histidines were deprotonated at high pH. For each of these 12 simulations, the starting structure was generated with all (ϕ , ψ) angles of an ideal α -helix (-60° , -40° , respectively). The simulations contained 2050 ± 100 waters.

Molecular dynamics simulations were conducted as described in the accompanying paper (Kirshenbaum & Daggett,

[†] This work was supported by Alzheimer's Disease Research, a program of the American Health Assistance Foundation, Rockville, MD.

* To whom correspondence should be addressed [telephone, (206) 685-7420; Fax, (206) 685-3252; E-mail, daggett@fitz.mchem.washington.edu].

[‡] Present address: Department of Pharmaceutical Chemistry, University of California, San Francisco, CA 94143.

[®] Abstract published in *Advance ACS Abstracts*, April 15, 1995.




pH State Modeled: H-bond present?	Distance from O of Ser 8 to Closest O of Glu 11, Average of last 100 ps	Conformational Consequence	Cartoon of Mainchain, and Residues 8 & 11
High pH Glu ionized H-bond present	Ser 8 OG to Glu 11 OE1 2.45 Angstroms	kink introduced at residues 8 & 9 helix maintained in residues 3 to 7	
Medium pH Glu ionized H-bond present	Ser 8 OG to Glu 11 OE1 2.45 Angstroms	kink in residues 8 & 9, helix then unfolds in res. 1 to 7 to satisfy the many electrostatic interactions at this pH	
Low pH Glu protonated no H-bond	Ser 8 OG to Glu 11 OE2 7.59 Angstroms	helix stable for 500 ps throughout entire length of peptide	

FIGURE 1: Overview of the putative Ser–Glu cap-induced conformational properties of the $\beta(1-28)$ peptide as determined by molecular dynamics simulations.

Table 1: Summary of Simulations Performed and Their Average Helix Content^a

peptide sequence ^a	pH	average helical content (%)
wild type	low	99
	medium	68
	high	83
Ser 8 → Ala	low	99
	medium	98
	high	88
Gly 9 → Ala	low	99
	medium	96
	high	95
Glu 11 → Gln	low	99
	medium	84
	high	97
Glu 11 → Asp	low	99
	medium	86
	high	87

^a The starting conformations contained 100% α -helical structure for all simulations, and the average values are for the 400–500 ps portion of each simulation.

1995). All simulations were performed at 298 K in water with periodic boundary conditions. An 8 Å nonbonded cutoff radius was employed, and the nonbonded list was updated every five steps. The time step for molecular dynamics was 2 fs, and atomic coordinates were saved every 100 steps (every 0.2 ps). The simulations were performed for 500 ps. Trajectories were monitored primarily by analysis of the extent to which the initial α -helical secondary structure was maintained, using a method described by Daggett et al. (1991). A segment of the peptide was defined to be helical when the (ϕ , ψ) angles of at least three consecutive residues were consistent with helical parameters ($-100^\circ \leq \phi \leq -30^\circ$, $-80^\circ \leq \psi \leq -5^\circ$) (Daggett et al., 1991; Daggett & Levitt, 1992), and noncontiguous helical segments were allowed.

RESULTS

Conformational Properties of the Wild-Type $\beta(1-28)$ Peptide. Elucidation of the mechanism of helix unfolding was facilitated by identifying those residues that showed a large fluctuation of (ϕ , ψ) dihedral angles away from helical parameters early in the simulation, concurrent to the start of the conformational transitions of interest. This analysis was performed at medium and high pH, as the peptide remained entirely helical at low pH (Table 1). For the high pH simulations, this analysis showed substantial rearrangement

of the main chain around the amide group of Gly 9 (the fluctuation in ψ_8 was 31° and 30° for ϕ_9 during the first 200 ps of the simulation, in contrast to values of approximately $10-15^\circ$ for the other residues). The rotation around Gly 9 took place as a rapid transition approximately 15–25 ps into the simulation. Visualization of the peptide structure revealed that this movement allowed the amide group of residue 9 to come into proximity with the hydrogen-bonded Ser 8–Glu 11 pair. As a result, the distance between the amide hydrogen of Gly 9 and the nearest carboxylate oxygen of the Glu 11 decreased from 5.9 Å in the starting structure to 3.7 Å, averaged over the last 100 ps of the simulation. In addition to providing a favorable interaction between these groups, this rearrangement alleviated the charge repulsion between the carboxylate and the main-chain carbonyl oxygen of Gly 9 (distance 8O to 11O_{ε1} increased from 3.7 to 5.2 Å). Movement of the main chain around residue 9 similarly allowed the amide nitrogens of Tyr 10 and Glu 11 to become significantly closer to the carboxylate charge site (6.1 to 4.3 Å for Tyr 10; 4.3 to 3.3 Å for Glu 11). The introduction of a kink into the peptide structure also stabilized the peptide by swinging the main-chain oxygens of residues 4–7 away from the negatively charged Glu 11, which would otherwise lie near the end of the N-terminal helix.

The creation of a “cap” between residues 8 and 11 upon ionization of the side-chain carboxyl groups interrupted the helical structure at this point in the sequence. By rotation of the dihedrals around Gly 9, the high pH structure was able to accommodate this cap by inserting a kink into the peptide with a minimal disruption of the secondary structure [Figures 2 and 3 of Kirshenbaum and Daggett (1995)]. The net result was two helices, both stabilized at their N-termini by the presence of an acidic residue. The larger C-terminal helix from residues 10 to 28 was stabilized by interaction with Glu 11. The smaller N-terminal helix from residues 3 to 7 was stabilized by the presence of Glu 3.

Analysis of the mean fluctuation of the ϕ and ψ angles for the first 200 ps of the simulation of $\beta(1-28)$ at medium pH revealed more substantial motion of the main chain than seen at high pH conditions. The movements at ψ_8 and ϕ_9 were similar to those seen at high pH and were interpreted as corresponding to the same influence of the Ser 8–Glu 11 cap. These dihedrals showed the same rapid transition to nonhelical parameters, although this process occurred later in the simulation.

The novel feature at medium pH was the very large mean fluctuation of ψ_6 and ϕ_7 (53° and 41° , respectively, for 0–200 ps). The rotation of these bonds was gradual and took place between 40 and 120 ps into the simulation, which was similar to the time frame in which the secondary structure of the N-terminus was lost [Figure 1 of Kirshenbaum and Daggett (1995)]. Residue 6 is a positively charged histidine residue, which suggests that the difference in behavior of the main chain at this site in comparison to the high pH simulation may be attributed to the influence of the imidazolium group. The presence of the Ser 8–Glu 11 cap resulted in the loss of helical structure at residues 8 and 9 (Figure 2). This established a helix terminus at this location and created a site of local positive charge density due to the presence of non-hydrogen-bonded amide groups. The subsequent movement about residues 6 and 7 extended the peptide backbone. This rearrangement increased the distance between His 6 and the region of positive charge density at the helix terminus (now beginning at residue 10), while allowing Asp 7 to reorient itself closer to this site. The presence of positively charged histidine residues at positions 13 and 14 at medium pH may have strengthened these interactions.

The main-chain rotation around His 6 prompted the loss of secondary structure in the remainder of the N-terminal region. As the side chain of Asp 7 moved closer to the helix terminus at residue 10, it also drew closer to the carboxylate group of Glu 11, where it eventually assumed the unusual water-bridged structure described in the accompanying paper [Figure 6 of Kirshenbaum and Daggett (1995)]. This movement placed Asp 7 into the peptide axis and further disrupted the ability of the N-terminal residues to maintain their helical geometries. Repulsive interactions between Asp 7 and the main-chain oxygens at residues 3–5 were the likely cause of further movement of the N-terminal region away from the 8–11 cap; the average distance between the two regions increased by over 2 Å at medium pH. As $\beta(1-28)$ became further extended in this region, water molecules were able to penetrate and find hydrogen-bonding partners along the backbone. The peptide carbonyl and amide groups rotated away from intramolecular α -helix hydrogen-bonding partners to interact with solvent, and the remaining secondary structure in the N-terminal region was lost.

On the basis of the disruption of the helical structure observed for the wild-type peptide, Ser 8, Gly 9, and Glu 11 appear to play important roles in the conformational transitions this peptide undergoes. Therefore, they represent good targets for computational mutagenesis studies.

Substitution of Serine 8 by Alanine. As observed for the native $\beta(1-28)$ peptide, molecular dynamics of S8A at low pH established an entirely helical structure that was stable throughout the 500 ps time course of the simulation (Table 1). The repeating α -helical content averaged for all structures generated over the last 100 ps was 99%. The structural features of S8A were essentially unchanged from those seen for the native peptide, including the side-chain orientations. This result established that the isosteric mutation did not significantly perturb the simulated conformation under conditions in which the peptide would not be expected to undergo unfolding.

At medium pH, however, the unfolding observed in the wild-type peptide was completely abolished (Figures 2B and 3). A hydrogen-bonded pair could not be established

between the side chains of residues 8 and 11, and the simulation yielded a structure that was 98% helical (Table 1). The alignment of acidic residues Glu 3, Asp 7, and Glu 11 along one face of the peptide seen at low pH was maintained upon deprotonation of the carboxyl groups. The introduction of a nonpolar side chain at position 8 allowed the creation of a hydrophobic cluster between Phe 4, Ala 8, and Val 12.

Deprotonation of the histidine groups at high pH resulted in the creation of a kink in the helix at positions 8 and 9 with subsequent loss of local helical structure (Figures 2B and 4). The repeating helical content for the peptide also, naturally, decreased as a result of the kink (Table 1). As with the native peptide, the kink was introduced in the first 50 ps by rotation of ψ_8 and ϕ_9 , thus permitting the main-chain carbonyls to move away from the carboxylate of Glu 11. Inspection of the final structure generated showed that Asp 7 and Glu 11 are now disposed on opposite sides of the helix, alleviating the electrostatic repulsion between these groups.

Substitution of Glycine 9 by Alanine. The G9A mutation resulted in retention of high helical content at all pH values, despite the fact that Ser 8 and Glu 11 were unaltered (Figure 2C). Only slight fraying at the N-terminus was observed (Figure 2C). The replacement of Gly by the bulkier Ala residue inhibited distortions of the main chain near residue 9 (Table 2) that are important in enabling Ser 8 and Glu 11 to come into close contact. In addition, this substitution replaces a residue with low helical propensity with one of high propensity.

Substitution of Glutamate 11 by Glutamine. Simulation of E11Q at low pH resulted in a stable helix throughout the trajectory (Table 1). At medium pH, a tight hydrogen-bonded pair was formed between the side chains of Gln 11 and Ser 8, as observed in the wild-type peptide. This was the only simulation in this series of mutations to show the presence of the 8–11 hydrogen bond. The distance between $8O_\gamma$ and $11O_\epsilon$ averaged over the final 100 ps was 2.7 Å, similar to the corresponding distance in the native peptide, 2.5 Å. The result of this hydrogen bond was to introduce a kink into the helix at residues 8 and 9 (Figure 2D). The helical content over the final 100 ps was 84%, corresponding to the loss of helical parameters at the kink and near the N-terminus (Figure 3). The side chain of Asp 7 did not swing down toward the helix axis to interact with the hydrogen-bonded pair, as observed for the wild-type peptide at medium pH. Glu 3 and Asp 7 remained extended from the helix and in proximity.

The Ser 8–Gln 11 hydrogen bond was severed at high pH. The result was an intact helical peptide throughout the simulation, with 97% helical content over the last 100 ps. In the place of the 8–11 interaction, Ser 8 was found to hydrogen bond with the main-chain carbonyl of Phe 4, and Gln 11 formed a hydrogen bond with the side chain of Gln 15 (distance at 500 ps: 2.4 Å from $4O$ to $8O_\epsilon$, 3.1 Å from $11N_{\epsilon 2}$ to $15O_{\epsilon 1}$). The formation of the Gln 11–Gln 15 interaction was facilitated by the movement of His 14 toward His 13, which would be energetically disfavored at medium pH. The absence of the serine cap and the decrease of electrostatic repulsion between acidic side chains obviated the necessity for a kink to form in the N-terminus and allowed the E11Q peptide to retain an entirely helical structure at high pH.

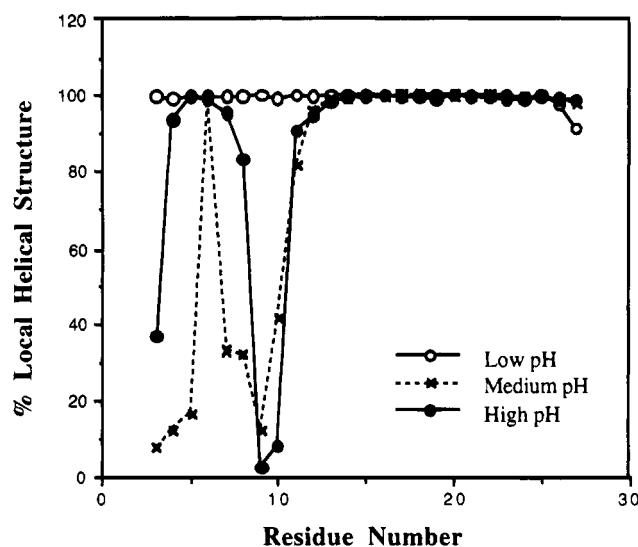
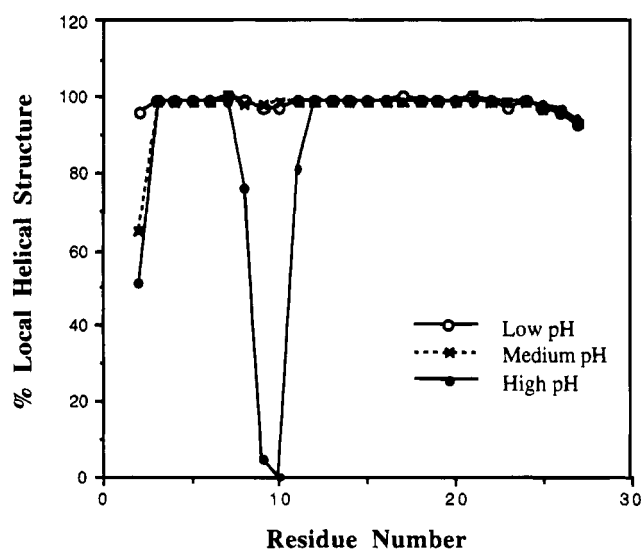
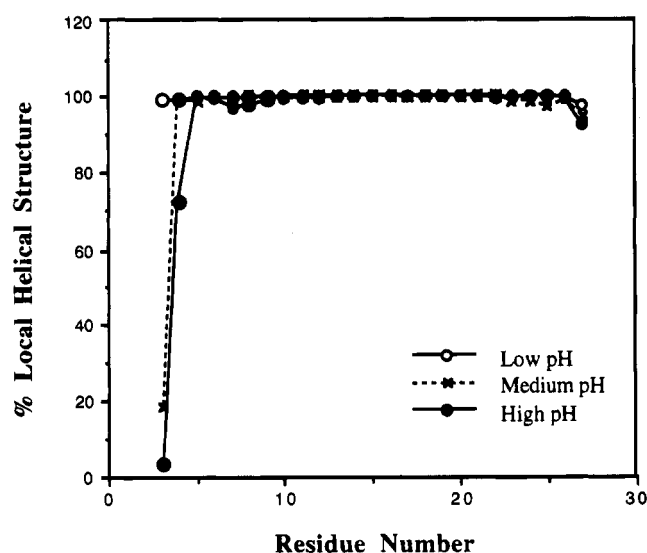
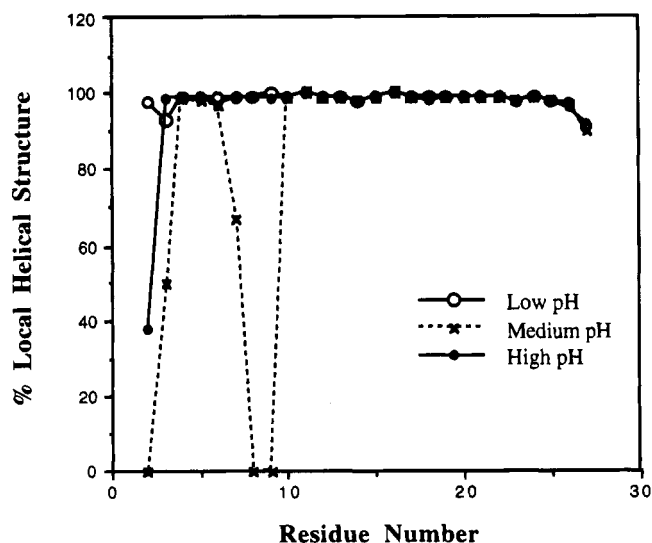
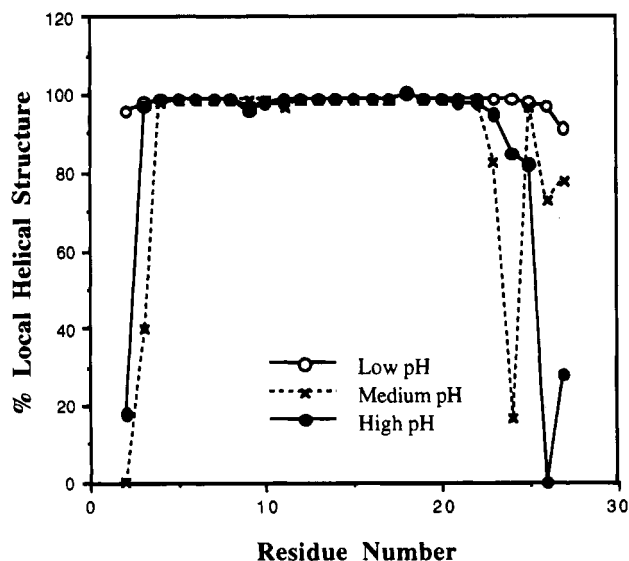
A. Wild type Peptide**B. S8A Mutation****C. G9A Mutation****D. E11Q Mutation****E. E11D Mutation**

FIGURE 2: Percentage of local α -helical structure as a function of residue number.

Substitution of Glutamate 11 by Aspartate. As observed for all simulations of the β -peptide at low pH, the initial

α -helical structure was maintained throughout the simulation (Table 1). The carboxyl group of Asp 11 was found to form

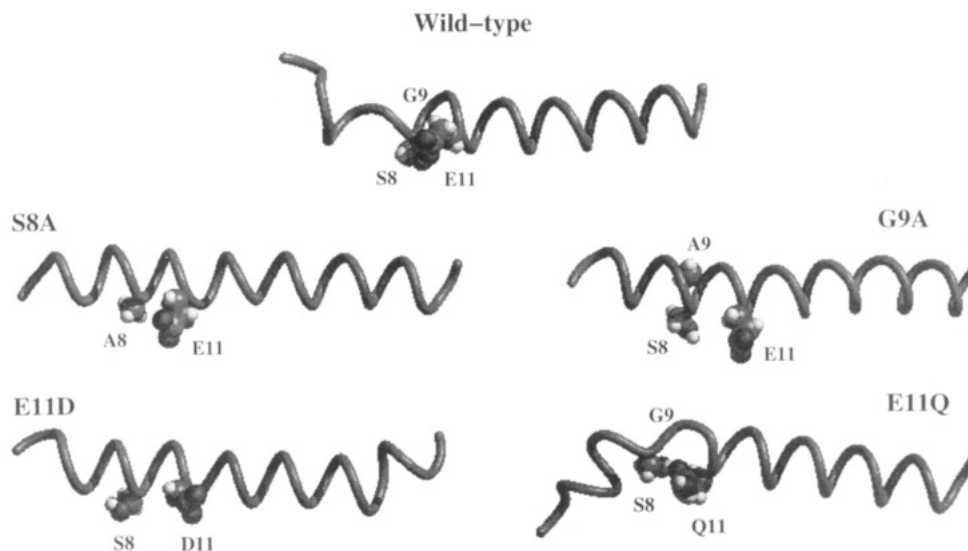


FIGURE 3: 500 ps snapshots from the simulations showing the effect of mutation on the conformation of the β -peptide at medium pH.

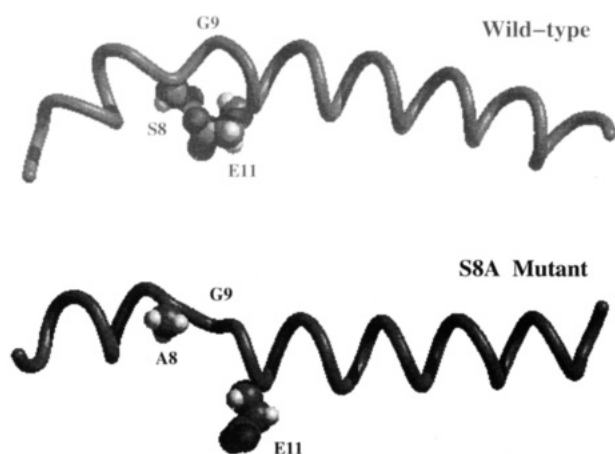


FIGURE 4: 500 ps snapshots from high pH simulations of the wild-type and S8A mutant peptides.

Table 2: Average Main-Chain Dihedral Angles for Residue 9^a

peptide sequence ^a	pH	ϕ_9 (deg)	ψ_9 (deg)
wild type	low	-57 (10)	-50 (11)
	medium	-102 (31)	-47 (11)
	high	-158 (13)	-33 (16)
Ser 8 \rightarrow Ala	low	-53 (10)	-46 (11)
	medium	-59 (10)	-55 (9)
	high	72 (20)	48 (18)
Gly 9 \rightarrow Ala	low	-63 (10)	-42 (11)
	medium	-62 (9)	-40 (9)
	high	-67 (10)	-38 (9)
Glu 11 \rightarrow Gln	low	-62 (12)	-48 (11)
	medium	-144 (14)	-30 (13)
	high	-57 (11)	-45 (12)
Glu 11 \rightarrow Asp	low	-51 (10)	-49 (9)
	medium	-34 (10)	-67 (11)
	high	-48 (9)	-47 (10)

^a The average values are for the 400–500 ps portion of each simulation, and the standard deviations during the time period are given in parentheses.

a close association with the amide group of Gln 15. The relative alignment of the acidic side chains of residues 3, 7, 11, and 22 along one face of the helix was not altered by the mutation.

The trajectory of the E11D simulation at medium pH yielded a predominantly helical conformation over the initial 200 ps. Some secondary structure was lost in the ensuing

200 ps, and the helical content over the final 100 ps was 86%, similar to that found for the E11Q simulation. However, the location of the loss of secondary structure was unexpected. A kink was not established, and the helix remained intact at residues 8 and 9. In addition to the reduced helical content in the N-terminus (residues 2 and 3), as had been observed previously, helical content was also diminished near the C-terminus (Figures 2E and 3).

Hydrogen bond formation between the side chains of Ser 8 and Asp 11 was not observed (the relevant distances were ≥ 8 Å). Ser 8 formed a hydrogen bond to the main-chain carbonyl group of Phe 4, and Asp 11 was oriented toward the C-terminus to interact with the side chain of His 14. The unfavorable electrostatic interactions between the acidic residues at positions 1, 3, 7, and 11 were accommodated by the extension of Asp 1 into solution rather than by rearrangements around residues 8 and 9 as observed for other simulations; this resulted in the loss of helical parameters at residues 2 and 3.

An additional noteworthy feature was the creation of a close contact between the negatively charged side chains of Glu 22 and Asp 23 (3.8 Å from 22O_{δ1} to 23O_{δ1}, averaged over last 100 ps). Examination of solvent structure at this site showed the presence of two water molecules that remained in a bridging conformation between the carboxylate groups, in an arrangement similar to that described between Asp 7 and Glu 11 in the wild-type β (1–28) simulations at medium pH (see accompanying paper). The hydroxyl group of Ser 26 was found to form a hydrogen bond to the main-chain carbonyl of Ala 21, and the amide group of Asn 27 formed a hydrogen bond to the main-chain carbonyl at residue 23. These structural rearrangements may be accommodated by the main-chain flexibility afforded by Gly 25.

As observed at medium pH, E11D gradually lost helical structure beyond 200 ps into the simulation at high pH, and the loss of secondary structure occurred at the N- and C-termini. The average helical content over the last 100 ps was 87%. Again, a hydrogen bond was not observed between Asp 11 and Ser 8. Ser 8 retained a hydrogen bond to the main chain of Phe 4. The deprotonation of His 14 resulted in the loss of the close contact between this residue and Asp 11 that was established at medium pH. The interaction between the side chains of Asp 22 and Glu 23

was also disrupted at high pH (minimum average distance between side-chain oxygen atoms 7.6 Å). The pattern of nonhelical parameters observed for the high pH simulation was somewhat different than observed at medium pH, with the majority of secondary structure loss occurring closer to the C-terminus (residues 24–27; see Figure 2E).

DISCUSSION

The accompanying study revealed that molecular dynamics simulations of the $\beta(1-28)$ amyloid peptide were able to reproduce the experimentally observed pH dependent conformational behavior of this peptide (Zagorski & Barrow, 1992). CD and NMR measurements detected the loss of α -helical structure in the N-terminal portion of the β -peptide above pH 3; increasing the pH above 7 resulted in the partial recovery of helical structure. Zagorski and Barrow (1992) suggested that electrostatic interactions between the acidic residues Glu 3, Asp 7, Glu 11, and Glu 22 could drive the structural rearrangements as these groups became charged. However, they recognized that the repulsive energies alone were probably insufficient to produce the observed unfolding and could not be invoked to understand the increased stability of the α -helix above pH 7. Our studies suggest that electrostatic repulsion between these acidic residues does not drive α -helix unfolding. Instead, these side chains became closer at medium pH in the simulations. We found that at medium and high pH an hydrogen bond was created between the side chains of Ser 8 and Glu 11; at medium pH Asp 7 also interacted with Glu 11. This "capping box" displaced charged groups into the helix axis and allowed water to form hydrogen bond partners with main-chain atoms, disrupting the helical structure in the N-terminal region of the peptide. At high pH, Asp 7 remained extended, and the Ser–Glu cap was accommodated by kinking the peptide with a minimal disruption of helical content outside of the region containing residues 7–10.

The simulation of peptide analogs of $\beta(1-28)$ with mutations at residues 8, 9, and 11 has allowed for further elucidation of the mechanism by which these residues contribute to the pH-dependent conformations exhibited by the peptide. We need to stress that these simulations of mutants were undertaken with a specific purpose in mind, to investigate the proposed mechanism of unfolding of the N-terminus of the $\beta(1-28)$ peptide when in the helical conformation. The mutations investigated have corroborated our earlier findings as well as providing more detailed information regarding the nature of the conformational transition. However, these results cannot necessarily be compared directly to experiment, as was done for the wild-type peptide. In studies of the wild-type peptide we found that consideration of a conformational ensemble was necessary for comparison to experiment, and this issue becomes even more critical when different mutants are compared. For example, there is no reason to think that the conformational population will remain the same upon mutation or that the mutation will not have an effect on the unfolded state. Therefore, we can say nothing about stability or overall structural tendencies of the mutant peptides; however, the approach is useful for specific investigation of the effect of different residues/interactions on the mechanism of unfolding of the α -helix.

The substitution of Ser 8 by alanine abolishes the presence of a capping interaction between residues 8 and 11 at medium

and high pH. Correspondingly, an all α -helical structure is maintained at medium pH, in marked contrast to the unfolding observed of the N-terminal third of the native $\beta(1-28)$ peptide under these conditions. The presence of a large number of acidic residues in the N-terminal segment of $\beta(1-28)$ does not inherently lead to conformational transitions upon ionization of the side-chain carboxyl groups. In the case of $\beta(1-28)$ this electrostatic repulsion may be mitigated by the presence of a large number of basic residues in this region. In fact, upon going to high pH, the neutralization of histidine residues results in kinking of the peptide, allowing acidic side chains to move apart. It is notable that these results indicate that it is possible to dramatically alter the simulated pH-dependent conformational properties of a peptide by introducing a residue that is not ionized over the conditions studied.

The substitution of Gly 9 by Ala introduces a residue of higher helical propensity into the peptide as well as restricting conformational freedom. This mutation, like that of S8A, abolished the Ser–Glu capping interaction and the pH dependence of the helix content, although in this case both residues are retained. Thus, the substitution to Ala appears to introduce a barrier to conformational transitions necessary to accommodate the Ser–Glu cap, as well as stabilizing the helical state. So, in addition to the role outlined for the Ser–Glu cap, one could view the local loss of helical structure in the wild-type peptide as being due to the presence of Gly 9. NMR experiments have documented a large local drop in helical structure at and around Gly residues in model helical peptides (Lyu et al., 1991).

The results of the E11Q simulation further establish the importance of the capping box in determining secondary structure. When the cap is present at medium pH, a kink is established at this site. When the cap is broken, at low and high pH, the peptide is entirely helical. Unfolding of the N-terminal portion of the helix at medium pH is not observed, demonstrating that the presence of the cap alone in the absence of electrostatic repulsive forces generated by Glu 11 is insufficient to drive the larger structural rearrangements observed in the native peptide.

As noted above, an all-helical conformation is obtained at medium pH by the S8A and G9A mutations that eliminate the capping box. However, alanine is known to have a high propensity to be found in α -helical regions of protein structures, especially at mid-helical positions (Richardson & Richardson, 1988). Consequently, retention of helical structure in the S8A simulation may be due to more than just the absence of the capping box. Simulation of the E11D mutant allows for perturbation of the capping box without substantially altering the anticipated proclivity of the peptide to form a helix. The excision of the methylene group from the side chain of Glu 11 dramatically alters the nature of the peptide dynamics. The diminished length of the aspartate side chain reduces the conformational flexibility at this residue sufficiently that the formation of a hydrogen bond to Ser 8 cannot be established. Accordingly, the helical structure in the N-terminus was intact at all pH states. However, the marked influence of this mutation on the structural characteristics in the C-terminal region is unexpected, inasmuch as this site is 13 residues removed from the site of substitution in a linear peptide. It is especially noteworthy because the force field utilized a nonbonded cutoff of 8 Å, and these sites are greater than 16 Å apart.

This observation is validated by ongoing studies in which a mutation at Glu 22 results in structural alterations in the N-terminal region (data not shown).

Overall, the pH-dependent conformational behavior of the $\beta(1-28)$ peptide is exquisitely sensitive to modifications in primary sequence. Removal of a methylene group or mutations in a nonionizable side chain can severely perturb the structure. These results validate conclusions based on the molecular dynamics studies of the native peptide; this behavior is not an artifact of the technique employed but pertains to interactions mediated by the specific sequence of the $\beta(1-28)$ peptide.

Furthermore, these findings substantiate the suggested mechanism of the pH-dependent conformational behavior of the native peptide. The presence of the capping box necessitates a kink to be introduced into the helix axis. In the native peptide, both Asp 7 and Glu 11 form part of the capping box; the presence of two charged groups in the helix axis drives the further unfolding of residues 3–7. The E11Q simulation demonstrates that the capping and electrostatic properties must play a mutual role in driving the loss of helical structure throughout the N-terminal region.

Analysis of the amino acid sequences at the ends of helical segments of X-ray crystal structures has suggested that certain residues tend to initiate or terminate helical structure (Richardson & Richardson, 1988; Presta & Rose 1988). The stabilizing interaction of polar side chains with main-chain heteroatoms at helix termini that would otherwise lack hydrogen bond partners has been well characterized and termed "helix capping" (Serrano & Fersht, 1989). In particular, Harper and Rose (1993) have found that the sequence Ser-X-X-Glu is typical of a pattern that occurs frequently at the N-termini of helices. This "capping box" can initiate helical structure by allowing reciprocal bonding between the side-chain oxygen atoms and main-chain amide groups of the Ser and Glu residues. This Ser-X-X-Glu sequence is consistent with the helix N-terminus at residues 8–11 in the molecular dynamics simulations of the $\beta(1-28)$ peptide at medium and high pH. However, the simulations generate structures in which the bonding is side chain to side chain rather than the "normal" arrangement of side-chain–main-chain interactions, but the net effect is the same. Hammen et al. (1995) have recently presented evidence for a very stable side-chain–side-chain hydrogen bond between a Thr and Asp, albeit in a different structural context.

Recently, CD and 2-D NMR spectroscopies have been used to characterize the solution structure (pH 5.5–6) of short (20 residue) helical peptides containing the Ser-X-X-Glu sequence (Lyu et al., 1993; Zhou et al., 1994). The NOESY spectrum of one of these peptides demonstrated that the Glu side chain formed a stable structure consistent with the reciprocal side-chain–main-chain interactions proposed by Harper and Rose. The region around this capping box displays a severe kink in the peptide axis, such that the helix cannot propagate. Thus, these authors concluded that the capping box both initiates and terminates helices; it stabilizes the N-terminus of the helix while simultaneously precluding the propagation of helical structure beyond this point by kinking the peptide. However, Jimenez et al. (1994) have recently demonstrated that a capping box does not necessarily prevent propagation of helices when stabilizing interactions exist with neighboring residues.

The molecular dynamics simulations of the $\beta(1-28)$ peptide and mutant analogs are in agreement with many of these features. The simulations show that in the presence of interactions between Ser 8 and the side chain of Glu 11, the helical structure at this point is interrupted by a kink. The helix C-terminal to this site is very stable and does not show evidence of fraying. When this interaction is disrupted, either by protonation of Glu 11 at low pH or by mutations at these residues that preclude the interaction at medium pH, such as S8A or G9A, helical structure may be retained throughout the region. The simulations do not demonstrate the presence of side-chain–main-chain interactions at this site; the side chains of residues 8 and 11 form a hydrogen bond. The discordance between this finding and the NMR structure is likely due to the influence of the neighboring residues. Residue 9 in the $\beta(1-28)$ peptide is a glycine, and the movement of Glu 11 toward Ser 8 appears to be possible only with the increased rotational freedom around Gly 9.

The importance of the Ser 8–Glu 11 interaction in driving the simulated pH-dependent conformational transitions immediately suggests that experimental detection of the capping box may be a pH-dependent phenomenon. The protonation of carboxylate groups involved in such interactions may help to generate large conformational changes in protein structure in response to alterations of pH.

The finding from the E11D simulation that mutation of a residue near the N-terminus influences the pH-dependent behavior of the C-terminus at a distance much greater than the nonbonded cutoff radius suggests that the modeling of long-range interactions may be possible, even with a short cutoff. The influence of the mutation appears to occur through the propagation of motion down the helix axis, an effect that may be accentuated by the presence of side-chain–main-chain capping interactions at the C-terminus (work in progress).

In any case, our results indicate that "simulated mutational analysis" may be of general utility for elucidation of the manner in which critical residues mediate peptide structure and dynamics. Such an approach may assist in *de novo* design of peptides and proteins and could identify critical amino acid targets for protein engineering. In the present study it has demonstrated the importance of the interaction between Ser 8 and Glu 11 in establishing the pH-dependent conformational properties of the helix \rightarrow coil transition of the $\beta(1-28)$ peptide at its N-terminus.

ACKNOWLEDGMENT

We thank Michael Zagorski for many helpful discussions. Some of this work was performed at Reed College as part of an undergraduate thesis (K.K.), and we gratefully acknowledge the faculty of the Chemistry Department, especially Tom Dunne, Alan Shusterman, and Arthur Glasfeld, for making this possible and for valuable suggestions.

REFERENCES

- Barrow, C. J., & Zagorski, M. G. (1991) *Science* 253, 179–182.
- Barrow, C. J., Yasuda, A., Kenny, P. T. M., & Zagorski, M. G. (1992) *J. Mol. Biol.* 225, 1075–1093.
- Daggett, V., & Levitt, M. (1992) *J. Mol. Biol.* 223, 1121–1138.
- Daggett, V., & Kirshenbaum, K. (1995) *Biopolymers* (submitted for publication).
- Daggett, V., Kollman, P. A., & Kuntz, I. D. (1991) *Biopolymers* 31, 285–304.

- Hammen, P. K., Scholtz, J. M., Anderson, J. W., Waygood, E. B., & Klevit, R. E. (1995) *Protein Sci.* (in press).
- Harper, E., & Rose, G. D. (1993) *Biochemistry* 32, 7605–7609.
- Jimenez, M. A., Muñoz, V., Rico, M., & Serrano, L. (1994) *J. Mol. Biol.* 242, 487–496.
- Kirshenbaum, K., & Daggett, V. (1995) *Biochemistry*, 34, 7629–7639.
- Lyu, P. C., Wang, P. C., Liff, M. I., & Kallenbach, N. R. (1991) *J. Am. Chem. Soc.* 113, 3568–3572.
- Lyu, P. C., Wemmer, D. E., Zhou, H. X., Pinker, R. J., & Kallenbach, N. R. (1993) *Biochemistry* 32, 421–425.
- Presta, L. G., & Rose, G. D. (1988) *Science* 240, 1632–1641.
- Richardson, J. S., & Richardson, D. C. (1988) *Science* 240, 1648–1652.
- Serrano, L., & Fersht, A. R. (1989) *Nature* 342, 296–299.
- Zagorski, M. G., & Barrow, C. J. (1992) *Biochemistry* 31, 5621–5631.
- Zhou, H. X., Lyu, P., Wemmer, D. E., & Kallenbach, N. R. (1994) *Proteins: Struct., Funct., Genet.* 18, 1–7.

BI941977H